SOLID MATTER

ELECTRONIC PROPERTIES OF (111) SURFACE IN A^3B^5 AND A^2B^6 CRYSTALS

T.V. GORKAVENKO,[1] S.M. ZUBKOVA,[2] V.A. MAKARA,[1] L.N. RUSINA,[2] O.V. SMELYANSKY[2]

[1]**Taras Shevchenko National University of Kyiv, Faculty of Physics**
(64, Volodymyrs'ka Str., Kyiv 01601, Ukraine; e-mail: gorka@univ.kiev.ua)

[2]**I.M. Frantsevych Institute for Problems of Materials Science, Nat. Acad. of Sci. of Ukraine**
(2, Krzhyzhanivs'kyi Str., Kyiv 03680, Ukraine; e-mail: svzubkova@ukr.net)

The electronic band structure, the local densities of states (the total and layer-resolved ones), and the distribution of charge density of valence electrons at the (111) polar surface in A^3B^5 and A^2B^6 crystals, such as GaAs and ZnSe, have been studied. The properties of anion- and cation-terminated surfaces have been analyzed separately. The self-consistent "3D" pseudopotential method has been used for numerical calculations in the framework of a model of layered superlattice. The application of an original iterator in the self-consistence procedure allowed difficulties associated with the surface-induced presence of reciprocal-lattice vectors shorter that 1 a.u. to be overcome.

1. Introduction. A Short Review of Researches of the Electronic Structure of (111) Surface in Crystals of the A^2B^6- and A^3B^5-types with Sphalerite and Wurtzite Structures

To study the surface states, three main methods are usually applied [1]: the bond-orbital, tight-binding, and self-consistent pseudopotential ones. The first method was used in the 1970s to calculate the properties of (111) surface in the elementary semiconductors Si and Ge. However, it found no wide application [2].

The non-self-consistent tight-binding method was proposed for the first time by Slater and Koster in 1954 [3]. In work [4], it was applied to calculate the electronic structure of (001) surfaces for all types of surface reconstructions known from experimental data, as well as for perfect (110) and (111) surfaces of cubic silicon carbides. The authors of work [4] marked that the tight-binding

method describes well the valence band, but unsatisfactorily the conduction band and the energy gap. They also obtained the total and the layer-resolved density of states for various types of β-SiC (001) surface reconstructions.

Five different configurations of polar β-SiC (001) surfaces were calculated in work [5] from the first principles. The calculations were carried out within the self-consistent method, by using of smooth separable norm-conserving pseudopotentials in the local-density approximation of density-functional theory.

A similar method was used to calculate the surface energies and to predict types of the reconstruction of actual surfaces of various bulk phases of zirconium oxide ZrO_2.

In work [6], the self-consistent pseudopotential calculations for (110) surfaces in semiconductors of the A^2B^6 and A^3B^5 types with the zinc-blende structure – ZnSe and GaAs – were carried out for the first time within the layered-superlattice model. In contrast to the case of polar (111) surface, the atoms of both types are on (110) surface. The calculation confirmed the validity of experimental results obtained for GaAs specimens by photoemission, energy loss spectroscopy, ellipsometry, and other techniques that testify to the existence of two surface states associated with dangling bonds. It was shown that (110) surface is semiconducting.

For the GaAs (110) surface, only the relaxation of gallium and arsenic surface atoms was observed [7]. At the same time, on the GaAs (001) one, there exists a wide spectrum of structures depending on the chemical com-

position of the surface layer and the means of surface preparation. In work [8], the atomic and electronic structures of four structural reconstructions of a GaAs (001) − (4 × 2) gallium-terminated surface were studied within the pseudopotential method and the layered-superlattice model. The surface and local electron densities of states, band spectra, and relative surface energies of those structures were calculated.

In work [9], the surface energetics of elementary semiconductors Ge, Si, and diamond with various types of the reconstruction – 1 × 1, 2 × 1, $c(4 \times 2)$, $c(2 \times 8)$, and 7 × 7 – of (100), (110), and (111) surfaces was studied from the first principles on the basis of the pseudopotential method with a plane-wave basis. The total energies and the corresponding band structures were determined. The behavior of various reconstructions was analyzed in terms of atomic sizes and orbital energies.

In recent years, a large attention has been attracted to the analysis of surface characteristics and interfaces in indium nitride, a narrow-gap semiconductor with $E_{gap} \approx 0.65$ eV that reveals the ability to maximally accumulate electrons on a pure InN (0001) surface fabricated by the molecular beam epitaxy method; this phenomenon is not observed for the majority of III–V compounds. It was experimentally found that electrons create a separate subband in this accumulating InN (0001) layer. The alloy of InN with the wide-band-gap semiconductor GaN ($E_{gap} \approx 3.4$ eV) opens new capabilities in band engineering [10, 11].

Along with the study of electronic and optical properties of the ground state of crystal surfaces in the framework of density-functional theory, the researches of excited surface states were started with the use of the many-particle perturbation theory. The corresponding calculations have already been made for two-dimensional systems based on the IV-group elements, e.g., for the pure surfaces of silicon and graphene, as well as for the C (111) 2 × 1 surface [12, 13].

The densities of states – total and in separate layers – at perfect (111) surface of A^2B^6 and A^3B^5 semiconductors with the zinc-blende structure were studied in the AlP compound using the bond-orbital method [2], in GaAs and ZnSe using the tight-binding method [14], and in GaN using the linear combination of atomic orbitals method [15].

In this work, to study the electronic structure of the (111) surface of similar crystals, we applied a "three-dimensional" self-consistent pseudopotential method within the layered-superlattice model that was used for the first time in work [16] in the silicon (111) surface researches. In this case, a solid state surface is simulated as a layered superlattice, i.e. a system of thin films that includes 5 to 20 and even more atomic layers that are periodically alternate in the direction perpendicular to the surface, being separated by vacuum intervals. The thickness of a vacuum gap was selected so that the interaction between neighbor films can be neglected.

This model is much more convenient than the model of semiinfinite crystal, because the artificially induced three-dimensional translational symmetry in the direction perpendicular to the crystal surface allows one to use well-developed "three-dimensional" methods for the calculation of the surface electronic structure.

The (111) surface of A^2B^6- and A^3B^5-type compounds with the sphalerite structure is a special case of polar surface, when the atoms of only one sort – either a cation or an anion – are located on the surface. The polar surface can be imagined as alternating parallel planes that contain atoms of only one sort. The atomic layers form hexagonal plane lattices in the [111] direction that are separated by the intervals of 1/4, 1/12, 1/4, 1/12, 1/4.... Here, the enhancement of ionic bond degree at changing from one compound to another, i.e. the increase of bond asymmetry, is the major factor, which governs features of the electronic energy structure. In our case of periodically arranged films with an even number of atomic layers, a cation and an anion lie on the opposite film surfaces.

2. Application of Layered-superlattice Model to the Calculation of Electronic States at (111) Surface of ZnSe and GaAs Crystals with Sphalerite Structure

A big prolate elementary cell is so selected that, in two dimensions, it is determined by the shortest vectors of the direct lattice; i.e., for a hexagonal lattice, these are vectors $a\sqrt{2}/2$ in length each, where a is the crystal lattice constant. In the third dimension, we select the c-axis, which passes in the [111] direction as the large diagonal of the cube (in such a way, the cubic structure of sphalerite is regarded as a hexagonal one) and extends over M atomic and N empty layers. The numbers M and N are chosen as follows: i) the film has to possess a sufficient thickness so that the interaction between both its surfaces could be neglected, and ii) the surface potential has to damp in "vacuum", so that other periodically located films could not affected it. The test calculations gave the values $M = 12$ and $N = 4$; therefore, we obtained $c = 5a\sqrt{3}/2$. The choice of 12 atomic layers guarantees that the plate contains an integer number of irreducible crystal layers. In the case of perfect (111)

surface, those layers include six atomic layers of each type.

Hence, the problem consists in a self-consistent calculation of the electronic structure of a "periodic" system, in which a hexagonal cell contains 12 atoms in the case of a nonreconstructed structure.

The wave function is expressed as a linear combination of plane waves with the wave vectors equal to the reciprocal lattice vectors,

$$\psi_{\mathbf{k}}^n(\mathbf{r}) = \sum_{\mathbf{G}} a_{\mathbf{k}}^n(\mathbf{G}) e^{i(\mathbf{k}+\mathbf{G})\mathbf{r}}, \tag{1}$$

where n enumerates the bands.

The system of equations to be solved by the iteration procedure has a standard form,

$$\sum_{\mathbf{G}} \left(H_{\mathbf{G},\mathbf{G}'} - E\delta_{\mathbf{G},\mathbf{G}'} \right) a_{\mathbf{k}}(\mathbf{G}) = 0, \tag{2}$$

where

$$H_{\mathbf{G},\mathbf{G}'} = |\mathbf{k}+\mathbf{G}|^2 \delta_{\mathbf{G},\mathbf{G}'} + V_{\mathrm{ps}}(\mathbf{G},\mathbf{G}'). \tag{3}$$

The calculations were carried out with the use of 1017 plane waves, which corresponds to the choice $|\mathbf{G}_{\max}|^2 \le 4.8$ a.u.

The procedure of self-consistent iteration was started from the empirical pseudopotential

$$V_{\mathrm{emp}}(\mathbf{G}) = S(\mathbf{G}) V_{\mathrm{emp}}^{\mathrm{at}}(|\mathbf{G}|), \tag{4}$$

where

$$S(\mathbf{G}) = \frac{1}{M} \sum_{\tau_i} e^{-i\mathbf{G}\boldsymbol{\tau}_i} \tag{5}$$

is the structural factor which describes an atomic arrangement in the "large" elementary cell, and the values for the form factors $V_{\mathrm{emp}}^{\mathrm{at}}(|\mathbf{G}|)$ were obtained from the continuous curve [17]

$$V(q) = \frac{a_1(q^2 - a_2)}{e^{a_3(q^2 - a_4)} + 1}. \tag{6}$$

Four parameters a_i were determined by fitting the dependence $V(q)$ to known form factor values for a bulk crystal; afterwards, they were renormalized to a different volume of the elementary cell. The renormalization consisted in multiplying the form factors by the "old" elementary cell volume that is equal to $3a^3/4$, and dividing the result by the "new" volume, $2 \times \frac{a^2\sqrt{3}}{8} \times \frac{5\sqrt{3}a}{2} = 15a^3/8$. The form factors for "new" $\mathbf{G}$-vectors of the

surface problem were obtained by a continuous extrapolation of expression (6).

The solution of Eqs. (2) and (3) for eigenvalues and eigenfunctions gave the energies $E_n(\mathbf{k})$ and the pseudowave functions that are determined by Eq. (1). Those quantities were calculated at 28 points of the irreducible $(1/12)$ two-dimensional hexagonal Brillouin zone. Such a relatively large number of points for $\mathbf{k}$ (instead of a single $\mathbf{k}$-point or a few "special" $\mathbf{k}$-points, as is often done) was chosen in order to determine the Fermi level and the charge of valence electrons with an accuracy as high as possible.

The charge density of valence electrons was calculated at each iteration by the formula

$$\rho(\mathbf{r}) = e \sum_{\mathbf{k},n}^{\mathrm{Br.z.}} \Psi_{\mathbf{k}}^{n*}(\mathbf{r})\Psi_{\mathbf{k}}^n(\mathbf{r}), \tag{7}$$

where the summation over $\mathbf{k}$ and the energy band number n means that $\mathbf{k}$ belongs to the Brillouin zone and the energy $E_n(\mathbf{k}) < E_F$, respectively. After substituting Eq. (1) in Eq. (7), we obtain

$$\rho_n(\mathbf{r}) = e \sum_{\mathbf{k}} \left[\sum_m \left(a_{\mathbf{k}}^n(\mathbf{G}_m) \right)^2 + \right.$$

$$\left. + \sum_{i \ne j} a_{\mathbf{k}}^n(\mathbf{G}_i) a_{\mathbf{k}}^n(\mathbf{G}_j) \cos\left[(\mathbf{G}_i - \mathbf{G}_j)\mathbf{r} \right] \right]. \tag{8}$$

The Fermi level that corresponds to the maximal energy of valence electrons was also calculated at each iteration. Its convergence was one of the criteria for the convergence of the whole self-consistent iteration process.

Further, the dependence $\rho(\mathbf{r})$ served as a basis for the calculation of Hartree–Fock screening potentials V_H and V_X. The potential V_H is a repulsive Coulomb potential that describes the action of all other valence electrons on the given one. It is determined by the Poisson equation

$$\nabla^2 V_H(\mathbf{r}) = -4\pi e^2 \rho(\mathbf{r}) \tag{9}$$

and can be presented as a Fourier-series expansion

$$V_H(\mathbf{r}) = \sum_{\mathbf{G}} V_H(\mathbf{G}) e^{i\mathbf{G}\mathbf{r}}, \tag{10}$$

where

$$V_H(\mathbf{G}) = \frac{4\pi e^2 \rho(\mathbf{G})}{|\mathbf{G}|^2}. \tag{11}$$

The divergence of $V_H(\mathbf{G})$ at $\mathbf{G} \to 0$ has no physical meaning, because it is completely eliminated by the ionic potential induced by positive ions,

$$V_{\text{ion}}^{\text{at}}(q) = (b_1/q^2)[\cos(b_2 q) + b_3]e^{b_4 q^4}. \qquad (12)$$

The ionic potential was obtained by fitting the model atomic potential to the values of atomic terms, as was done by Heine and Abarenkov [18]. The quality of this potential was tested by carrying out the self-consistent calculations of the band structures in bulk ZnSe and GaAs. Therefore, we may put[1]

$$V_H(\mathbf{G} = 0) = V_{\text{ion}}(\mathbf{G} = 0) = 0.$$

In the framework of the Slater statistical exchange model, the local form for the Hartree–Fock exchange potential looks like

$$V_X(\mathbf{r}) = -3\alpha e^2 (3/8\pi)^{1/3} \rho^{1/3}(\mathbf{r}), \qquad (13)$$

where $\alpha = 0.79$, as was adopted in the calculations for the bulk. Only the valence electrons are taken into consideration.

The function $\rho^{1/3}(\mathbf{r})$ was determined at every point separately in a three-dimensional grid with $N = 21600$ $\mathbf{r}$-points in the elementary cell. The function $\rho^{1/3}(\mathbf{r})$ was converted into its Fourier transform

$$\rho^{1/3}(\mathbf{G}) = \frac{1}{N} \sum_{\mathbf{r}_i} \rho^{1/3}(\mathbf{r}_i)e^{-i\mathbf{G}\mathbf{r}_i}. \qquad (14)$$

The sum of two Hartree–Fock potentials, V_H and V_X, composes the electron screening potential:

$$V_{\text{screen}}(\mathbf{r}) = \sum_{\mathbf{G}} [V_H(\mathbf{G}) + V_X(\mathbf{G})]e^{i\mathbf{G}\mathbf{r}}. \qquad (15)$$

It is worth emphasizing that it is determined at each self-consistent iteration from the total valence charge.

T a b l e 1. Parameters a_i for the empirical potential at ZnSe and GaAs (111) surfaces (Ry)

No.	Ga	As	Zn	Se
1	1.22	0.35	6.70	0.23
2	2.45	2.62	1.50	3.39
3	0.54	0.93	0.67	0.73
4	−2.71	1.57	−4.71	2.20

[1] In the practice of numerical calculations, the divergences of the Hartree–Fock and ionic potentials at small lattice wave vectors break the stability of and complicates the process of self-consistent iterations while solving the surface problem numerically. This issue will be discussed below in more details.

The calculation (the self-consistence loop) begins from the input empirical potential (4), (5). Table 1 exhibits the values of parameters a_i for empirical input potentials. The potentials are normalized by the atomic volume that is equal to the volume of a new large elementary cell (16 layers) divided by the number of atoms in the cell (12), in particular, 190.2 a.u. for ZnSe and 188.7 a.u. for GaAs. The lattice constants for ZnSe and GaAs are 5.65 and 5.635 Å, respectively.

At a second iteration, the input potential is equal to the sum of ionic and screening potentials. Table 2 exhibits the values of parameters b_i for the ion-frame potential (12) at (111) surface of ZnSe and GaAs.

Hence, the input potentials for the first and second iterations in the self-consistence procedure look like

$$\begin{aligned} V_{\text{in}}^{(1)}(\mathbf{r}) &= V_{\text{emp}}(\mathbf{r}), \\ V_{\text{in}}^{(2)}(\mathbf{r}) &= V_{\text{ion}}(\mathbf{r}) + V_{\text{screen}}^{(1)}(\mathbf{r}). \end{aligned} \qquad (16)$$

Since the empirical potential $V_{\text{emp}}(\mathbf{r})$ for bulk crystals was used in the calculations, we did not obtain – as would be expected – a satisfactory screening charge on the surface after the first iteration. Really, the potential $V_{\text{in}}^{(2)}(\mathbf{r})$ gives rise to the spectrum of eigenvalues and the charge that strongly differ from the results of the first iteration with $V_{\text{in}}^{(1)}(\mathbf{r})$, and all the following steps of the self-consistence procedure did not make the results convergent.

The matter is that, in the problem for the bulk, the shortest vector in the reciprocal lattice has the length $2\pi(111)/a > 1$ a.u., whereas the length of such a vector in the problem for the surface is $2\pi/a_c < 1$ a.u. Here, c means the axis of a large elementary cell. For short vectors in the reciprocal lattice, $|\mathbf{G}| < 1$, the iterated system (16) is very unstable. Mathematically, this circumstance manifests itself in that the dependences $V_{\text{out}}(\mathbf{G}) = f(V_{\text{in}}(\mathbf{G}))$ for the reciprocal-lattice vectors within this interval are curves with a large slope (often negative); i.e. the smallest variations of the input potential (a few tenths or hundredths of eV) bring about the changes of both the order of the input potential and its sign.

T a b l e 2. Parameters b_i for the empirical potential of the ionic frame at ZnSe and GaAs (111) surfaces (Ry)

No.	Ga	As	Zn	Se
1	−0.34	−0.71	−0.31	−2.32
2	1.33	1.04	1.34	0.53
3	0.45	0.17	0.082	− 0.57
4	0.0071	−0.015	−0.0086	−0.032

In accordance with the results obtained by other authors [6, 7], the calculation of the input potential at the $(n + 1)$-th iteration as a linear combination of the input and output potentials at the n-th iteration does not provide the convergence. Therefore, to obtain the input potential $V_{\text{in}}^{(n)}(\mathbf{G})$ for $n > 2$, we studied the curves $V_{\text{out}}(\mathbf{G}) = f(V_{\text{in}}(\mathbf{G}))$ for every small $|\mathbf{G}| < 1$ a.u. separately and proposed the following iteration procedure. Let us draw a straight line in the coordinate system $(x = V_{\text{in}}(\mathbf{G}), y = V_{\text{out}}(\mathbf{G}))$ through two points (x_1, y_1) and (x_2, y_2) that correspond to the input and output, respectively, potentials for two iterations preceding to the iteration (x, y) under consideration. We obtain a system of equations

$$\frac{x_1}{a} + \frac{y_1}{b} = 1 \quad \text{and} \quad \frac{x_2}{a} + \frac{y_2}{b} = 1, \tag{17}$$

whence we can find the constants a and b:

$$a = \frac{x_2 y_1 - x_1 y_2}{y_1 - y_2}, \quad b = \frac{x_2 y_1 - x_1 y_2}{x_2 - x_1}. \tag{18}$$

The convergence of the procedure corresponds obviously to the equality $x \approx y$ between the input and output potentials. Therefore, from the system of equations ([22]), we obtain the following condition for the input potential in the current iteration:

$$x = \frac{ab}{a + b}, \tag{19}$$

In the literature, the input potential x (Eq. (19)) is often written down as a linear combination of the input and output potentials taken from the preceding iteration,

$$x = \alpha x_2 + (1 - \alpha) y_2, \tag{20}$$

where the coefficient of a linear combination of the input and output potentials from the preceding iteration (x_2, y_2) is equal to

$$\alpha = \frac{x - y_2}{x_2 - y_2}. \tag{21}$$

Expression (20) for the input potential allows the self-consistence process to be made controllable. Namely, the parameter α has to fall within the interval $0 < \alpha < 1$. This procedure was carried out for every iteration, starting from the third one, and separately for the real and imaginary parts of the potential.

Then, we calculated and analyzed the densities of states (total one and that in each layer) for cation- and anion-terminated surfaces:

$$N(E) = \sum_{\mathbf{k}_{ii}, n} \int_{\Omega} \left| \Psi_{\mathbf{k}_{ii}(\mathbf{r})} \right|^2 d\mathbf{r} \, \delta(E - E_n(\mathbf{k}_{ii})). \tag{22}$$
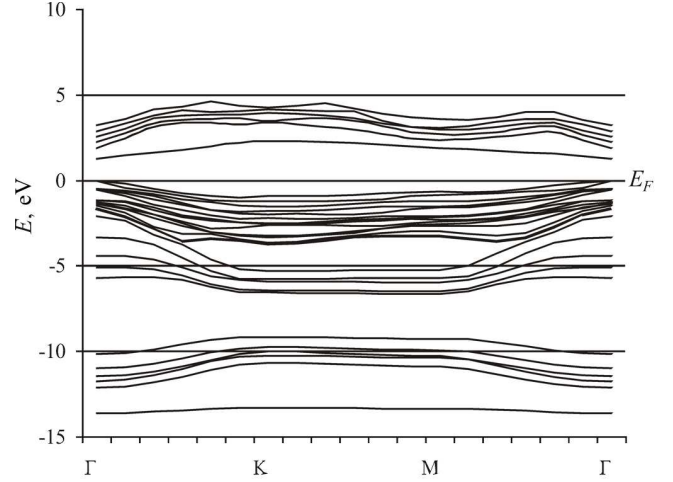
Fig. 1. Band structure of a 16-layer (111) GaAs film

Here, the integration is carried out over the volume of either a separate layer or the whole elementary cell. Expression (22) is interpreted as a probability for an electron with energy E to be found in volume (region) Ω.

The authors developed an AEPP software package, which allows one to obtain a self-consistent solution for a system of equations within the pseudopotential method with an original iterator, to calculate the dispersion laws at the surface in the framework of the layered-superlattice model, to calculate the total and layer-resolved densities of states, the 3D- and contour distribution maps for charge densities – total, for charges in separate energy bands, and at separate points in the Brillouin zone – and so on. The soft package can be used for an arbitrary crystal structure and arbitrary numbers of empty and filled atomic layers. It can be easily adapted for surfaces with various indices. The authors can easily improve the software package and expand its scope of applications.

3. Results of Numerical Experiment and Conclusions

3.1. Band structure and electron density of states

In this work, we calculated two-dimensional band structures, the total and layer-resolved densities of states, and the distributions of charge density created by valence electrons in ZnSe and GaAs (111) films. The convergence of iterations was achieved after 20 to 24 steps, until the input and output potentials differed by 0.1–0.15 eV from each other.
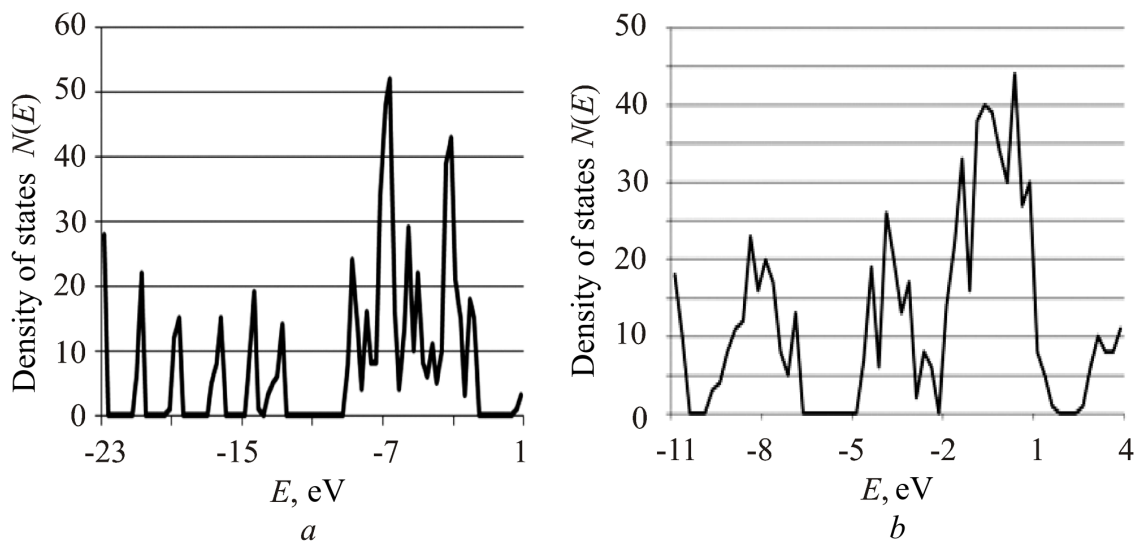
Fig. 2. Total densities of states in ZnSe (*a*) and GaAs (*b*) (111) films
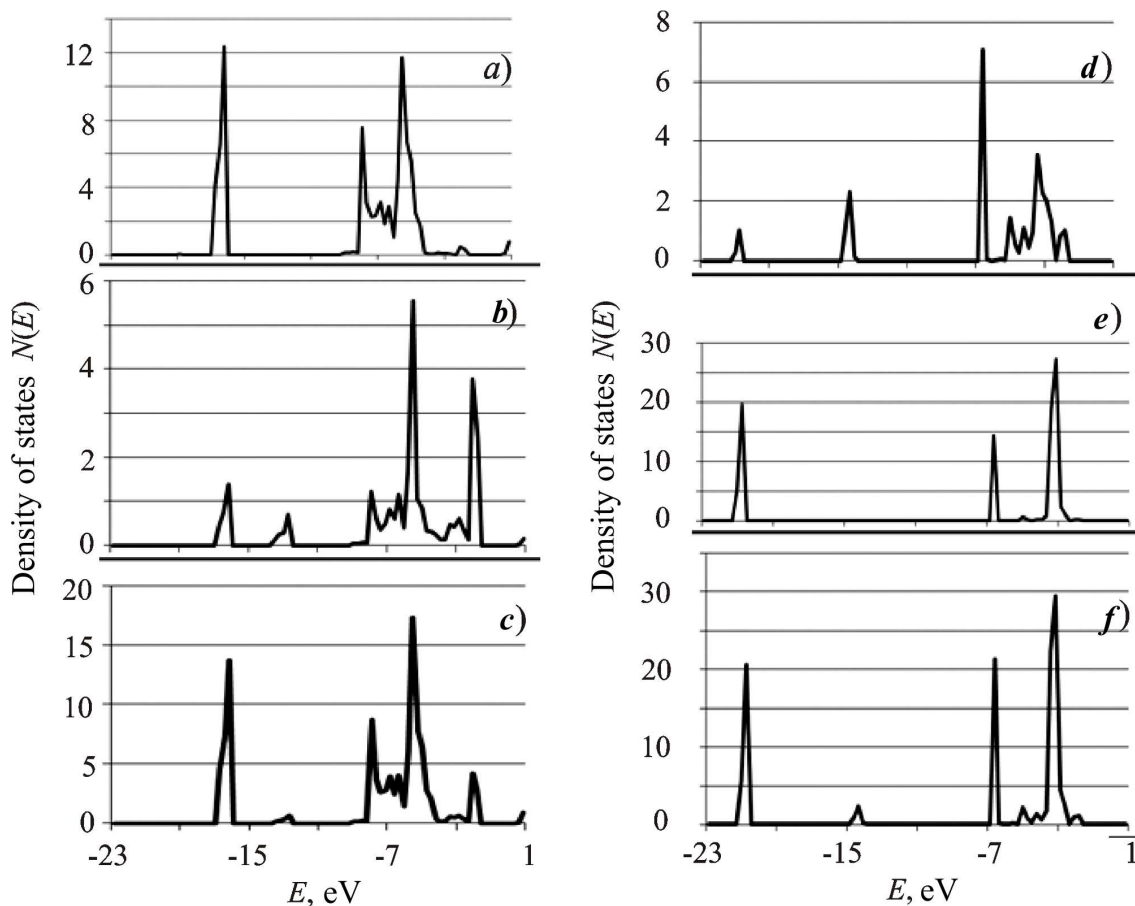
Fig. 3. Density of states in a Se-terminated ZnSe (111) film: (*a*) Se 6 atomic layer, (*b*) Zn 7 atomic layer, (*c*) (Se 6 + Zn 7) central molecular layer, (*d*) Zn 11 atomic layer, (*b*) Se 12 atomic layer, (*c*) (Zn 11 + Se 12) surface molecular layer
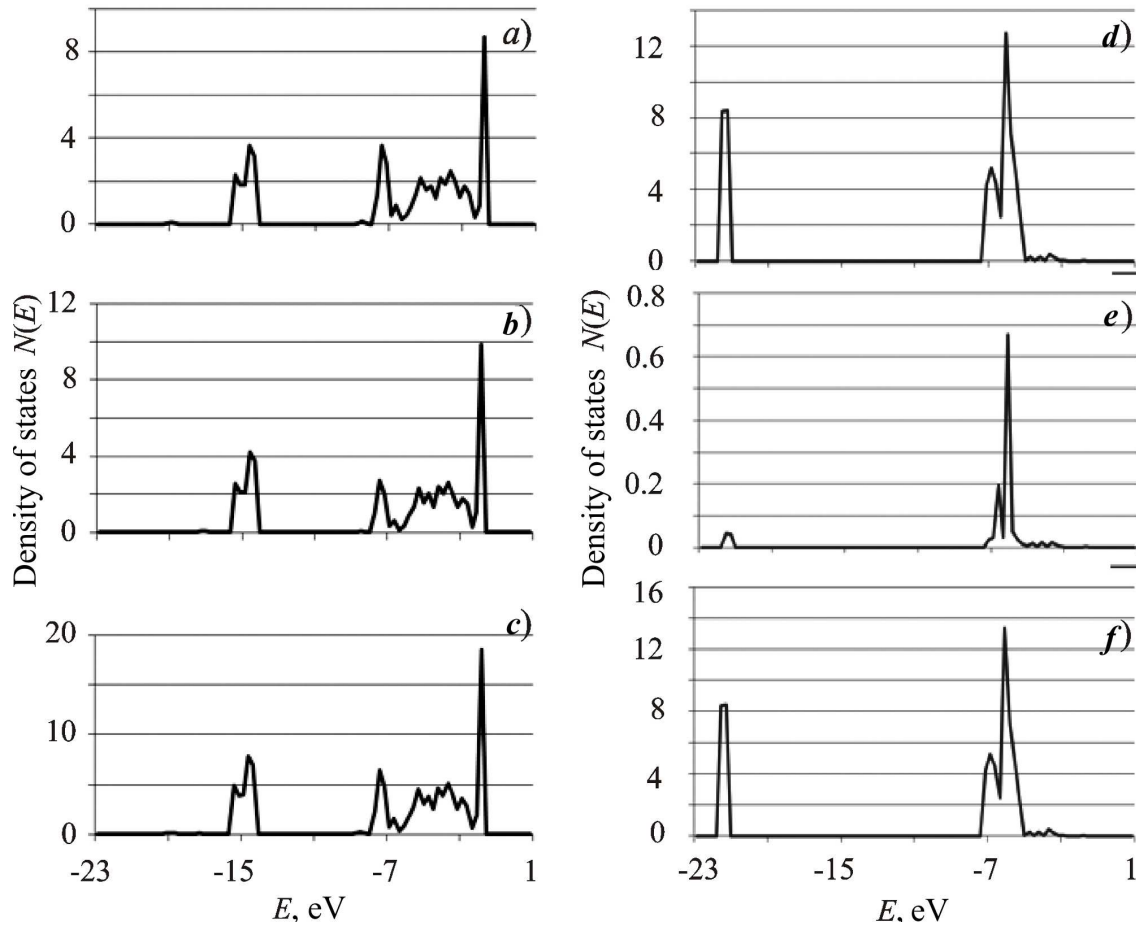
Fig. 4. Density of states in a Zn-terminated ZnSe (111) film: (*a*) Zn 6 atomic layer, (*b*) Se 7 atomic layer, (*c*) (Zn 6 + Se 7) central molecular layer, (*d*) Se 11 atomic layer, (*b*) Zn 12 atomic layer, (*c*) (Se 11 + Zn 12) surface molecular layer

The band structures of 16-layer $(\ldots 12\text{–}4\text{–}12\text{–}4 \ldots)$ ZnSe and GaAs (111) films were calculated for surface vectors $\mathbf{k}_{\parallel}$ between points $\Gamma(0,0)$, $\mathrm{M}(1/2,0)$, $\mathrm{K}(1/3,1/3)$, and $\Gamma(0,0)$ in the two-dimensional Brillouin zone. By the example of the band structure of a (111) GaAs film (Fig. 1), it is seen that the singularities of the obtained dispersion curves are similar to those of the band structure of a (111) Si film [16]. The Fermi level passes through the valence band top. In Fig. 1, we observe a sufficiently strong separation of lower unfilled states from the valence band bottom, which decreases significantly the energy gap [8]. At point Γ, the distance between the Fermi level and the separated band is equal to 1.3 eV. The same distance is between the surface level created by the dangling bond of a Ga ion and the valence band top in the case of a surface terminated by a Ga ion.

Figures 2 to 5 present the curves for the total and layer-resolved densities of states in the (111) films of zinc selenide and gallium arsenide plotted with a step of 0.2648 eV for ZnSe and 0.2725 eV for GaAs. The covered energy range includes the whole valence band, the forbidden gap, and some interval of the conduction band.

Figure 2,*a* demonstrates the total density of states in a ZnSe (111) film that consists of 12 filled and 4 empty layers and is terminated by a Se ion.

Figures 3,*a* to *c* illustrate the density of states in the sixth (Se 6) and the seventh (Zn 7) atomic, and the central (Se 6 + Zn 7) molecular layer, respectively, in such a 12-layer film. The central double layer is separated by five atomic layers from each of the film surfaces, and its density of states approaches the bulk value. It can be regarded as a projection of bulk density of states onto the (111) plane. The figures testify that, in the central layer, the contribution of a Se ion to the density of states in the depth of the valence band is an order of magnitude larger than that made by a Zn ion, whereas at the
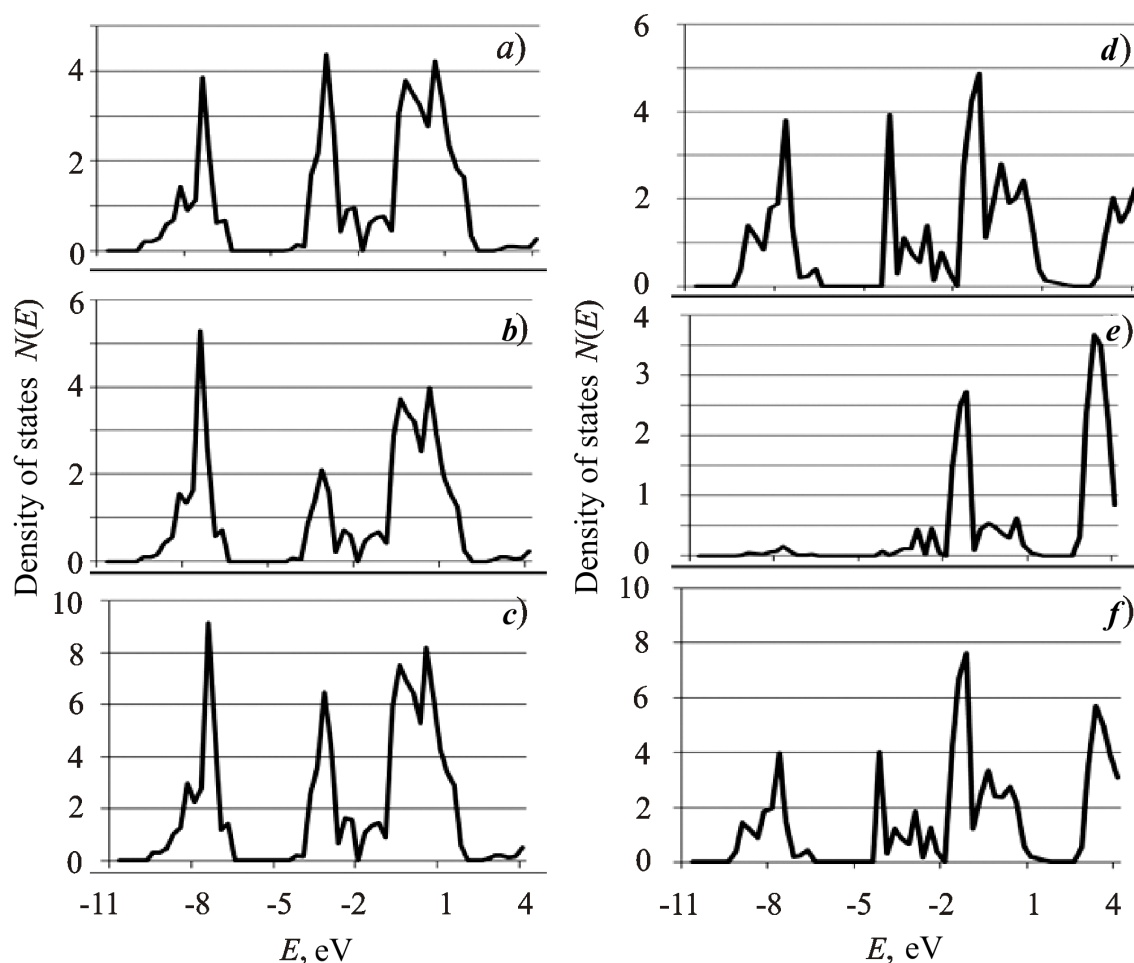
Fig. 5. Density of states in a Ga-terminated GaAs (111) film: (*a*) Ga 6 atomic layer, (*b*) As 7 atomic layer, (*c*) (Ga 6 + As 7) central molecular layer, (*d*) As 11 atomic layer, (*b*) Ga 12 atomic layer, (*c*) (As 11 + Ga 12) surface molecular layer

lower boundary of the fundamental energy gap, the contribution of a Zn ion is 7 to 8 times as large as that of a Se ion.

Figures 3,*d* to *f* exhibit the densities of states in the surface layer Se 12, the subsurface layer Zn 11, and the surface molecular layer Zn 11 + Se 12, respectively. A comparison of those figures testifies to the appearance of a large peak in the density of states (the maximal number of states is 20.6) at a distance of about 2 eV from the valence band bottom. This peak corresponds to a dangling bond of the surface Se ion. The second peak in the density of surface states is located at a distance of about 1 eV down from the valence band top (the maximal number of states is 29.5). Here, the contribution of a surface Se ion to the density of states is almost 8 times as large as the contribution of a subsurface Zn ion, the share of which amounts to about 13%.

In Figs. 4,*a* to *c*, the densities of states are shown for the atomic layers Zn 6 and Se 7, and the central molecular layer (Zn 6 + Se 7), respectively, in a 12-layer ZnSe film terminated by a Zn ion. In this case, the surface level induced by a dangling bond appears at a distance of about 1 eV above the valence band bottom (the maximal number of states is 8.4). The second surface level is located at a distance.of 6 eV under the valence band top (the maximal number of states is 13.4). The contribution of a Zn ion, at which the bond becomes broken, amounts to about 5%. In addition, weak resonances are observed in the conduction band.

Figures 4,*d* to *f* demonstrate the densities of states for the surface, Zn 12, and subsurface, Se 11, atomic layers and the surface molecular layer (Se 11 + Zn 12), respectively. A comparison between Figs. 2–4 makes it evident that the location and the arrangement of surface
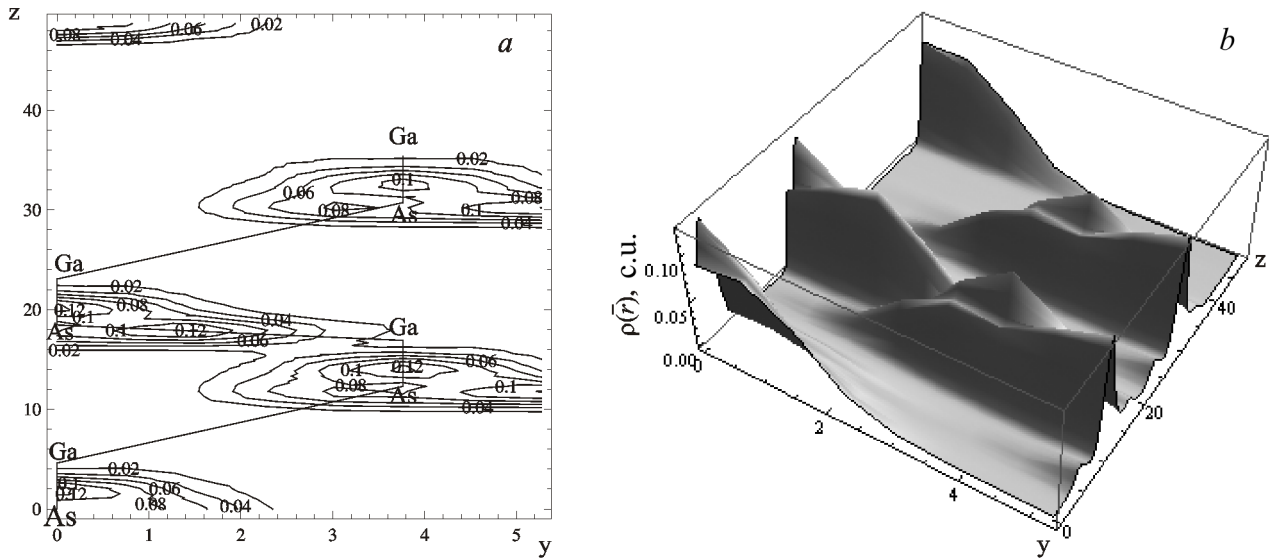
Fig. 6. Total valence charge density in a (111) film of the GaAs crystal terminated by a Ga ion: (*a*) – the contour plot, (*b*) – the 3D image
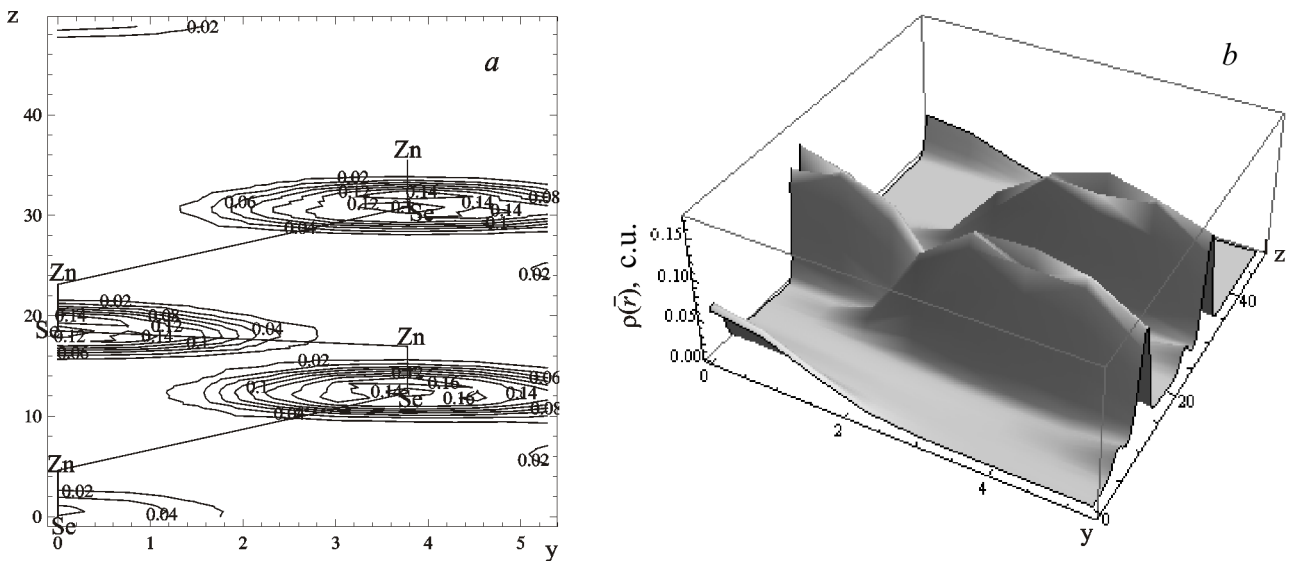
Fig. 7. Total valence charge density in a (111) film of the ZnSe crystal terminated by a Zn ion: (*a*) – the contour plot, (*b*) – the 3D image

levels depend on the atomic alternation in the surface molecular layer.

In GaAs, in contrast to ZnSe, the contributions of Ga and As ions to the density of states in the central molecular layer are comparable by magnitude – 42% by Ga and 58% by As ions, which is associated with a smaller difference between the ionicities of Ga and As atoms in comparison with that between Zn and Se ionicities.

In Fig. 2,*b*, the total density of states in a GaAs (111) film terminated by a Ga ion is shown.

Figure 5 exhibits the densities of states in a GaAs (111) film terminated by a Ga ion: panels *a* to *c* correspond to the Ga 6 and As 7 central atomic, and (Ga 6 + As 7) central molecular layers, respectively, whereas panels *d* to *f* to the As 11 and Ga 12 surface atomic, and (As 11 + Ga 12) surface molecular layers, respectively. One can see that, in the depth of the valence band at a distance of 3 eV from its top, there emerges a surface level induced by a dangling bond and created mainly by the As ion. At the same time, a surface level created

mainly by the dangling bond of a Ga ion is observed in the energy gap at a distance of about 1.3 eV from the valence band top.

A comparison of the studied properties for the density of states at (111) surface with the results of work [6] obtained for (110) surface in crystals with the zinc-blende structure demonstrates a substantial difference between them. This circumstance is explained, first of all, by the fact that there are atoms of both kinds on (110) surface, whereas only cations or anions are present on (111) one. The difference is observed between the band structures, local densities of states, and charge density maps (see below). In the case of GaAs (111) surface, the band induced by dangling bonds is located in the energy gap. The properties of (111) surface in sphalerite-type crystals are similar to those of silicon (111) surface.

As the ionicity increases, the energy level of the surface state decreases and enters the valence band.

3.2. Charge-density distribution for valence electrons

In the present work, we obtained the 3D images and the contour maps of charge-density distributions for valence electrons in a (111) film of the GaAs crystal. The film is started by an As (Ga) ion and terminated by a Ga (As) one. In Fig. 6,a, b, the results are illustrated by the example of a GaAs (111) film that is started by an As ion and terminated by a Ga ion. The contour map is represented in the $(1\bar{1}0)$ plane that intersects (111) plane at a right angle.

Here, as well as in the following figure, 8 atoms (4 atoms A and 4 atoms B) are located in the $(1\bar{1}0)$ plane that is normal to (111) surface. The z-axis corresponds to the c-axis of a large prolate elementary cell. The y-coordinates of points in the elementary cell are reckoned along the y-axis. The vertical axes in 3D plots correspond to the charge-density magnitude. The charge density is normalized by the number of electrons in the elementary cell and is expressed in terms of 10^{-3} a.u. (to make the notation compact, we write it as "c.u.").

In the chosen $(1\bar{1}0)$ plane, 4 atoms (2A + 2B) have the coordinate $x = 0$ and 4 atoms (2A + 2B) the coordinate $x = 3.765$ a.u. in the GaAs case and $x = 3.775$ a.u. in the ZnSe one. The average charge density is about 0.013 c.u. near the Ga ion and about 0.076 c.u. near the As one. The calculations show that the charge density in the upper surface layer in a (111) film of the GaAs crystal differs weakly from the charge density in the central layers.

In Fig. 7,a, b, the results are illustrated by the example of a (111) film of the ZnSe crystal that is started by an Se (Zn) ion and terminated by an Zn (Se) one, are shown. The calculations showed that the average charge density is about 0.003 c.u. near the Zn ion and about 0.106 c.u. near the Se one. The maximal charge density of about 0.16–0.18 c.u. is reached in the central film layers at a distance of about 0.7–0.9 a.u. from the Se ion, around which a considerable part of the valence charge is accumulated. It is clearly seen that the density of valence charge decreases asymmetrically toward the left and right film boundaries. The large humps are related with Se ions, and the small projections to Zn ones.

4. Conclusions

We have calculated and analyzed the total density of states for (111) films of ZnSe and GaAs that are composed of 12 filled and 4 empty layers and are terminated by a Se (Zn) or As (Ga) ion, respectively; the density of states of the central molecular layer (sixth and seventh atomic layers), and the densities of states of the surface and subsurface layers and the surface molecular layer (totally 26 versions). It turns out that the density of states of the central double layer separated by 5 atomic layers from each of the film surfaces approaches the bulk one. We can consider it as the projection of the bulk density of states on (111) plane. The locations and the arrangement of surface levels depends on the alternation of atoms in the surface layer.

In ZnSe, the contributions of Zn and Se ions to the density of states of the central molecular layer differ from each other by at least one order, whereas these contributions in GaAs are comparable: 42% and 58% for Ga and As, respectively, which is related to the less difference in the ionicities of Ga and As atoms as compared with those of Zn and Se ones. The calculations indicate that the charge density of the upper surface layer in a (111) film of the GaAs crystal differs slightly from that of central layers.

We have calculated the 3D images and the contour maps of charge-density distributions for valence electrons in a (111) film of the GaAs crystal that is started by an As (Ga) ion and is terminated by a Ga (As) one, as well as those in a (111) film of the ZnSe crystal that is started by a Se (Zn) ion and is terminated by a Zn (Se) one, respectively.

A tendency for the bond to be more ionic, when changing from GaAs to ZnSe, is obviously illustrated in the charge density plots. As it occurs in the crystal bulk, the valence charge increases around the anion and de-

creases around the cation, whereas the charge along the covalent bond between the ions diminishes.

The enhancement of bond ionicity gives rise to a quicker damping of surface perturbation in ZnSe, in comparison with that in GaAs. The matter is that the charge is mostly localized at the Se ion, which governs the behavior of the total charge density. Therefore, a strong Se potential can be considerably perturbed only at the upper surface level.

It is worth noting that (111) surface is not a cleavage plane for crystals of the zinc-blende type. For the creation of a polar surface, a large electrostatic energy is needed, which is necessary for two half-spaces with oppositely charged boundaries to be separated from each other. However, such a surface was obtained by bombarding those crystals with Ar^+ ions followed by their annealing under ultrahigh vacuum conditions. The specimens of gallium arsenide and gallium phosphide were used to carry out experiments on studying the surface and bulk contributions to electron photoemission spectra and the electron energy loss spectra [19], the low-energy electron diffraction [20], and the angle-resolved ultraviolet photoemission spectra [21]. The energy difference between the dangling Ga– and As– bonds for a perfect surface of gallium arsenide, which was obtained in this work, correlates with the energy difference between the corresponding peaks in the angle-resolved ultraviolet photoemission spectrum [22]. Unfortunately, no unreconstructed structures were found for the (111) surfaces of GaAs and ZnSe [23].

1. A. Zangwill, *Physics at Surfaces* (Cambridge University Press, Cambridge, 1988).

2. S. Ciraci, I.P. Batra, and W.A. Tiller, Phys. Rev. B **12**, 5811 (1975).

3. J.C. Slater and G.F. Koster, Phys. Rev. **94**, 1498 (1954).

4. Xiao Hu, Hong Yan, M. Kohyama, and F.S. Ohuchi, J. Phys.: Condens. Matter **7**, 1069 (1995).

5. M. Sabisch, P. Kruger, A. Mazur *et al.*, Phys. Rev. B **53**, 13121 (1996).

6. J.R. Chelicowsky and M.L. Cohen, Phys. Rev. B **13**, 826 (1976).

7. J.R. Chelicowsky and M.L. Cohen, Phys. Rev. B **20**, 4150 (1979).

8. S.E. Kul'kova, S.V. Eremeyev, A.V. Postnikov *et al.*, Izv. Vyssh. Ucheb. Zaved. Fiz. N 10, 44 (2006).

9. A.A. Stekolnikov, J. Furthmuller, and F. Bechstedt, Phys. Rev. B **65**, 115318 (2002).

10. P.D.C. King, T.D. Veal, P.H. Jefferson *et al.*, Appl. Phys. Lett. **91**, 092101 (2007).

11. T.D. Veal, P.D.C. King, and C.F. McConville, Phys. Rev. B **77**, 125305 (2008).

12. M. Marsili, O. Pulci, F. Bechstedt, and R. Del Sole, Phys. Rev. B **78**, 205414 (2008).

13. O. Pulci, P. Gori, V. Garbuio *et al.*, Phys. Status Solidi A **207**, 291 (2010).

14. D.J. Chady and M.L. Cohen, Phys. Rev. B **11**, 732 (1975).

15. B. Stankiewicz, L. Jurczyszyn, R. Kucharczyk, and M. Steslicka, Czech. J. Phys. **47**, 473 (1997).

16. M. Schluter, J.R. Chelicowsky, S.G. Louie, and M.L. Cohen, Phys. Rev. B **12**, 4200 (1975).

17. F. Bechstedt and R. Enderlein, *Semiconductor Surfaces and Interfaces* (Akademie-Verlag, Berlin, 1988).

18. J.D. Abarenkov and V.B. Heine, Philos. Mag. **12**, 529 (1965).

19. A.D. Katnani and D.J. Chadi, Phys. Rev. B **31**, 2554 (1985).

20. S.Y. Tong, G. Xu, W.Y. Hu, and M.W. Puga, J. Vac. Sci. Technol. B **3**, 1076 (1985).

21. A.D. Katnani, H.W. Sang, P. Chiaradia, and R.S. Bauer, J. Vac. Sci. Technol. B **3**, 608 (1985).

22. P.K. Larsen and J.F. van der Veen, J. Phys. C **15**, L431 (1982).

23. K. Oura, V.G. Lifshits, A.A. Saranin, A.V. Zotov, and M. Katayama, *Surface Science. An Introduction* (Springer, Berlin, 2003).

ЕЛЕКТРОННІ ВЛАСТИВОСТІ ПОВЕРХНІ (111) В A^3B^5 ТА A^2B^6 КРИСТАЛАХ

Т.В. Горкавенко, С.М. Зубкова, В.А. Макара, Л.М. Русіна, О.В. Смелянський

Р е з ю м е

Для полярної поверхні (111) в кристалах типу A^3B^5 і A^2B^6: GaAs, ZnSe досліджено електронну зонну структуру, локальну густину станів (повну та пошарову) та розподіл зарядової густини валентних електронів. Окремо розглянуто властивості поверхонь, що закінчуються катіоном та аніоном. Чисельний розрахунок проведено самоузгодженим "тривимірним" методом псевдопотенціалу в рамках моделі шаруватої надґратки. В процесі самоузгодження використано оригінальний ітератор, який дозволяє подолати труднощі, зумовлені наявністю, у випадку поверхні, векторів оберненої ґратки, менших 1 ат. од.